ARTICLE
Journal of Cellular Biochemistry 115:1787–1798 (2014)

Journal of Cellular Biochemistry

MCP-1 as a Potential Target to Inhibit the Bone Invasion by Oral Squamous Cell Carcinoma

Jingjing Quan,[1,2] Nigel A. Morrison,[2*] Newell W. Johnson,[3] and Jin Gao[4**]

[1]*Guanghua School of Stomatology, Hospital of Stomatology, Sun Yat-sen University & Guangdong Provincial Key Laboratory of Stomatology, Guangzhou, Guangdong 510055, China*

[2]*School of Medical Science, Griffith University, QLD 4222, Australia*

[3]*Griffith Health Institute, Griffith University, QLD 4222, Australia*

[4]*School of Dentistry and Oral Health, Griffith University, QLD 4222, Australia*

ABSTRACT

Bone invasion is a common complication of oral squamous cell carcinoma (OSCC), and this study sought to explore whether suppressed expression of monocyte chemotactic protein-1 (MCP-1) can be used to inhibit the bone invasion by OSCC. Strong staining of MCP-1 protein was observed from 10 archival blocks of OSCC by immunohistochemistry (IHC). Real-time PCR showed MCP-1 mRNA was highly expressed by OSCC cell lines (SCC25, HN5, and Tca8113), and SCC25 cells had the highest expression. An expression construct of a dominant negative variant of MCP-1 with 7 amino acids truncated (7ND), in the vector pcDNA was used to transfect SCC25 cells, and resultant stabilized SCC25 cells (SCC25-7ND) were generated by antibiotic selection. 10% conditioned media (CM, supernatant) of SCC25-7ND cells efficiently inhibited the formation of human osteoclasts grown from $CD14^+$ monocyte subpopulation, comparing with 10% CM of SCC25 cells. Further, cells of SCC25 or SCC25-7ND were injected onto the surface of calvariae of nude mice to establish an animal model of bone invasion by OSCC. H&E staining showed well-differentiated OSCC was formed in both groups, tumour cells invading the bone while osteoclasts locating in typical resorption lacunae. TRAP staining indicated significantly fewer osteoclasts were found in calvariae with cells of SCC25-7ND in comparison to cells of SCC25. These data demonstrate the relevance of MCP-1 with research on bone invasion by OSCC, and suggest the potential value of MCP-1 as a target to inhibit this common complication. J. Cell. Biochem. 115: 1787–1798, 2014. © 2014 Wiley Periodicals, Inc.

KEY WORDS: BONE INVASION; ORAL SQUAMOUS CELL CARCINOMA; MONOCYTE CHEMOTACTIC PROTEIN-1; OSTEOCLASTS

With the breakthrough of biological target therapy, treatment options for patients with bone destruction caused by cancer have been greatly expanded [Faccio, 2011]. A variety of treatments can be chosen now and biotherapy targeting on osteoclasts is a rational approach to reduce the risk for skeletal complications [Baron et al., 2011]. Since OSCC has the properties of bone invasion and osteoclasts play an important role in its progression [Quan et al., 2012b], finding an efficient target associated with osteoclasts for biotherapy is essential, which may enhance the therapeutic approaches in clinical management.

Chemokines (chemotactic cytokines) are a large family of small heparin-binding peptides, generally 70–90 amino acids in length [Balkwill, 2012]. According to the number and arrangement of serine residues, chemokines are segregated into four subfamilies—CXC, CC, C, and CX3C—, which have similar functions in terms of activation of leucocytes through their binding to selective receptors coupled with G-protein. To date, more than 50 chemokines and 20 chemokine receptors have been identified, which are known to play a crucial part in homing leukocytes and other cells in the human body, engendering both physiological and pathological processes [Charo et al., 2006].

Conflict of interest: none.

Grant sponsor: China Scholarship Council; Grant number: 2008638008; Grant sponsor: Sun Yat-sen University; Grant number: 13ykpy41; Grant sponsor: Griffith University Postgraduate Research Scholarship (GUPRS); Grant sponsor: National Health and Medical Research Council (NHMRC); Grant sponsor: Australian Dental Research Foundation (ADRF).

*Correspondence to: Dr. Nigel A. Morrison, School of Medical Science, Griffith University, QLD 4222, Australia. E-mail: n.morrison@griffith.edu.au

**Correspondence to: Dr. Jin Gao, School of Medicine & Dentistry, James Cook University, QLD 4870, Australia. E-mail: jin.gao@jcu.edu.au

Manuscript Received: 3 June 2013; Manuscript Accepted: 12 May 2014

Accepted manuscript online in Wiley Online Library (wileyonlinelibrary.com): 6 June 2014

DOI 10.1002/jcb.24849 • © 2014 Wiley Periodicals, Inc.

Monocyte chemoattractant protein-1 (MCP-1), also termed as chemokine (C-C motif) ligand 2 (CCL2), is one of the key members of CC chemokine family, which functions as a potent agonist for monocytes, dendritic cells, memory T cells and basophils [Taddei et al., 2012]. Note that MCP-1 is among the most thoroughly characterized members of the chemokine family; it has been shown to be a potential intervention point for the treatment of various diseases, such as multiple sclerosis, atherosclerosis, and rheumatoid arthritis [Deshmane et al., 2009]. Moreover, MCP-1 has been found to be overexpressed in several types of malignancy, and can mediate the osteoclastogenesis induced by neoplasms [Lu et al., 2009; Moreaux et al., 2011]. For example, using a xenograft model with SCID mice, Mizutani et al. reported overexpression of MCP-1 within the prostate cancer cell line, PC-3, enhanced the growth of bone metastases [Mizutani et al., 2009]. Histological analysis showed that increased numbers of functional osteoclasts were found in bone samples. To date, however, no report can be found concerning possible roles of MCP-1 for the invasion of bone by OSCC.

The progression of bone invasion by OSCC is a highly coordinated process, and may be divided into three phases: initial, resorption, and final phases [Quan et al., 2012a]. The main stage is the resorption phase, where osteoclasts play the key roles to degrade the bone matrix. Cytokines generated from malignant keratinocytes may directly or indirectly induce the formation of osteoclasts. Active osteoclasts are frequently observed in clinical tissue samples from OSCC patients with bone invasion, which usually appear in the edge of bone tissue and sit close to the neoplastic cells themselves. This phenomenon raises a specific question about how these osteoclasts are recruited or mobilized to the resorption sites. It also indicates the potential therapeutic value of blocking the messages which pass between malignant epithelial cells and osteoclasts, which may inhibit the progression of bone invasion by OSCC.

In addition to its expression in cancer cells, MCP-1 has also been identified as one of the typical chemokines associated with development and function of osteoclasts. Kim et al. reported that MCP-1 is induced by RANKL, where it accelerates the differentiation of human osteoclasts in an autocrine manner [Kim et al., 2005]. Furthermore, human peripheral blood mononuclear cells (PBMCs) treated by MCP-1 formed TRAP positive multinucleated osteoclast-like cells, but those cells were unable to resorb bone, indicating MCP-1 might promote osteoclast fusion, which is a key event of osteoclast differentiation [Kim et al., 2006]. With these reports, the aim of the present study is to investigate whether MCP-1 can be used to inhibit the bone invasion by OSCC via targeting on osteoclasts. An expression construct of a dominant negative variant of MCP-1 with seven amino acids truncated (7ND), in the vector pcDNA was used to transfect the OSCC cell line SCC25, and sought evidence of inhibiting effects both, in vitro and in vivo.

MATERIALS AND METHODS

REAGENTS

DMEM, Opti-MEM, foetal bovine serum (FBS), trypsin-EDTA, G418, and Alexa Fluor 594 (PE) conjugated secondary antibody were purchased from Life Technologies. α-MEM was obtained from Hyclone (Thermo Scientific). The primary polyclonal antibody of rabbit anti-human MCP-1 was obtained from Abcam, the other primary antibody of rat anti-mouse CD14 was obtained from eBioscience. The transfection reagent of FuGENE HD was got from Promega. Recombinant human cytokines of CSF1 and RANKL were purchased from Peprotech (Rocky Hill, NJ). The neutralization antibody against MCP-1 was purchased from R&D (Minneapolis, MN).

IMMUNOHISTOCHEMISTRY

To detect the expression of MCP-1 protein, 10 archival blocks were examined from 10 patients whose OSCC showed invasion of bone. Written informed consent was obtained from each patient, and approved by Australian Capital Territory (ACT) Heath Human Research Ethics Committee (ETHLR.11.137). Serial tissue sections (5 μm thickness) were dewaxed, rehydrated and treated with 0.3% hydrogen peroxide in PBS. Antigen retrieval was performed by heating sections in a microwave oven (2×4 min) in 0.2% citrate buffer (pH = 6.0). After non-specific binding was blocked with 5% BSA in phosphate buffered saline (PBS) for 30 min, sections were incubated with the primary antibody of MCP-1 (1:80) overnight at 4 °C. Sections were then treated with the anti-rabbit secondary antibody (Envision^{TM} + Systems) for 30 min, followed by diaminobenzidine (DAB) detection solution (Dako, Botany, Australia) for a few minutes at room temperature. The primary antibody was replaced by non-immune serum as negative controls. Sections were counterstained with Mayer's haematoxylin (Sigma), dehydrated, and mounted with DPX (BDH Laboratory, Poole, England). Osteoclasts were determined as giant cells with two or more nuclei (multinucleated), locating in typical bone resorption lacunae. The final results were visualized by light microscopy (Leitz Laborlux S, Germany) and photographed using an Olympus BX60 camera with CellSens software (Olympus, Japan).

CELL LINES AND CULTURE CONDITION

Normal epithelial cells (EP) and the prostate cancer cell line PC3 was supplied by Professor Jin Gao (James Cook University, QLD, Australia). The OSCC cell line SCC25 was a gift of Associate Professor Nick Saunders (Princess Alexandra Hospital, QLD, Australia). The OSCC cell lines HN5 and Tca8113 were kindly given by Professor Ming Wei (Griffith University, Australia) and Professor Qian Tao (Sun Yat-sen University, China) respectively. All cells were maintained in DMEM supplemented with 10% FBS and antibiotics (100 U/mL of penicillin G and 100 mg/mL of streptomycin, Invitrogen) at 37 °C in an incubator (5% CO_2/95% air).

REAL-TIME PCR

At the same time point, all cells were plated in 6-well plates at a density of 1×10^6 cells per well. After an overnight culture and when cells attained confluence, total RNA from each cell line was isolated using the PureLing RNA Mini Kit (Life Technologies). RNA was quantified and quality tested by spectrophotometry and gel electrophoresis. All samples were confirmed at 260/280 absorbance ratios between 1.8 and 2.1 and had prominent 18s and 28s bands. Thereafter, total RNA was converted into cDNA using ImProm-II Reverse Transcriptase (RT, Promega) and oligo dT primer (Promega).

Quantitative expressions of MCP-1 and 18S ribosomal RNA (rRNA) were performed using EXPRESS SYBR GreenER qPCR Supermix Universal Kit (Life Technologies). The primer sequences used to amplify 18S rRNA were 5′-CTTAGAGGGACAAGTGGCG-3′ and 5′-ACGCTGAGCCAGTCAGTGTA-3′; MCP-1 were 5′-TCGCGAGCTA-TAGAAGAATCA-3′ and 5′-TGTTCAAGTCTTCGGAGTTTG-3′. Thermal cycling was started at 95 °C for 2.5 min, followed by 45 cycles of amplification at 95 °C for 10 s, 58 °C for 10 s, 72 °C for 25 s and 72 cycles of elongation at 60 °C for 5 s as the final step. All reactions were carried out on the iCycler iQ5 real-time PCR system (Bio-Rad). The data were normalized to the internal control, 18S rRNA, to obtain ΔCt. The relative quantification of mRNA expression of MCP-1 gene was reported by the $2^{-\Delta\Delta Ct}$ method.

ESTABLISHING STABLIZED SCC25 CELLS WITH 7ND VECTOR BY CELL TRANSFECTION

An expression construct of a dominant negative variant of MCP-1 with seven amino acids truncated (7ND), in the vector pcDNA was kindly supplied by Associate Professor Kensuke Egashira (Kyushu University, Japan). FuGENE HD was used to mix 7ND, and the ratio between them was set as 1:3 (v/v) based on the optimization of previous studies. Briefly, cells of SCC25 were seeded into a 24-well plate at a density of 5×10^4 cells/well, with 500 μL of complete medium. After 24 h, the complete medium was changed into Opti-MEM, different amounts of 7ND (0.2 μg, 0.4 μg, 0.6 μg) were added to Opti-MEM respectively, to which the FuGENE HD was added to a final volume of 20 μL. This 7ND-FuGENE mixture was incubated

A

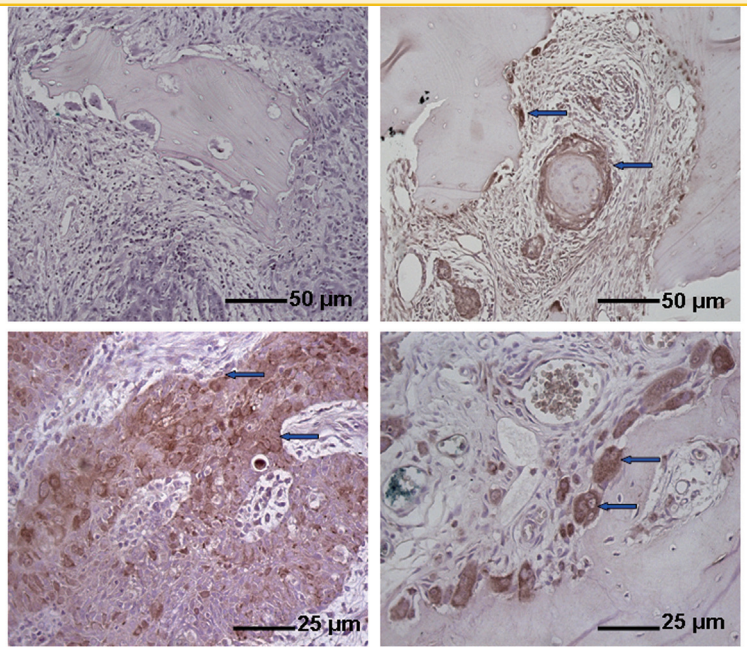

B

Case	Age	Sex	Site	Staining Density
1	53	M	mandible	+++
2	64	F	maxilla	++
3	76	F	mandible	+++
4	41	F	maxilla	+++
5	65	F	mandible	+++
6	70	F	mandible	+++
7	66	M	mandible	++
8	45	M	mandible	++
9	75	M	mandible	+++
10	76	M	maxilla	+

Fig. 1. Staining of MCP-1 protein in OSCC tissue samples with bone invasion. (A) MCP-1 protein was strongly stained in cytoplasm of osteoclasts and tumour cells (arrow, DAB, bar = 25/50 μm). Control sections showed negative staining (upper left, bar = 50 μm). (B) Summary of the staining results of all 10 samples.

for 15 min at room temperature to allow the transfection complex to form. Then the transfection complex was added dropwise to the cells. After 48 h, Opti-MEM was changed into complete medium and antibiotic selection of G418 was started. After approximately six days, the cultures were split in half and replated into 24-well plates. Antibiotic administration continued for another three weeks, at which time net growth was observed. Thereafter, the cells from three of the most resistant cultures were removed from the 24-well plate, pooled and then re-seeded by a one in two serial dilution in duplicate over two 24-well plates. After four days, these cells growing from a single colony were transferred to a new well in a 12-well plate. The cells were up-scaled further until they were grown in 25 cm^2 tissue culture flasks. These cells were then lysed, total RNA extracted, and cDNA was subsequently synthesized. Since primers of MCP-1 can amplify mRNA of 7ND, Real-time PCR was used to determine the relative gene expression of MCP-1 in all these cells, that with the greatest level of MCP-1 (SCC25-7ND) being used in the following studies.

$CD14^+$ MONOCYTES SEPARATION AND THE INDIRECT CELL CO-CULTURE

PBMCs were isolated from human blood collected into BD vacutainer cell preparation tubes (CPT) with sodium citrate (BD). After centrifugation at 1500 g for 30 min, the cell layer on top of the Ficoll-Paque in the CPT was collected, resuspended in 10 mL of α-MEM and re-centrifuged (1250 rpm, 10 min). Pure $CD14^+$ monocytes were extracted from PBMCs by incubation with MACS CD14 human microbeads (Miltenyi Biotec, Bisley, UK) for 15 min at 4 °C. Cells were washed by using $CD14^+$ isolation buffer (0.5% FCS; 2 mM EDTA, pH 8) and passed through an autoMACS magnetic cell separator. Then these $CD14^+$ monocytes were planted in 24-well plates at 1×10^5 cells/well in 600 μL of medium (α-MEM, pH 7.4, containing 10% FBS and 1% penicillin/streptomycin), with the recombinant human cytokines CSF1 (25 ng/mL) and RANKL (40 ng/mL) for generating the osteoclasts.

The indirect cell co-culture of $CD14^+$ monocytes and SCC25 cells was performed in 24-well culture plates, and groups were arranged

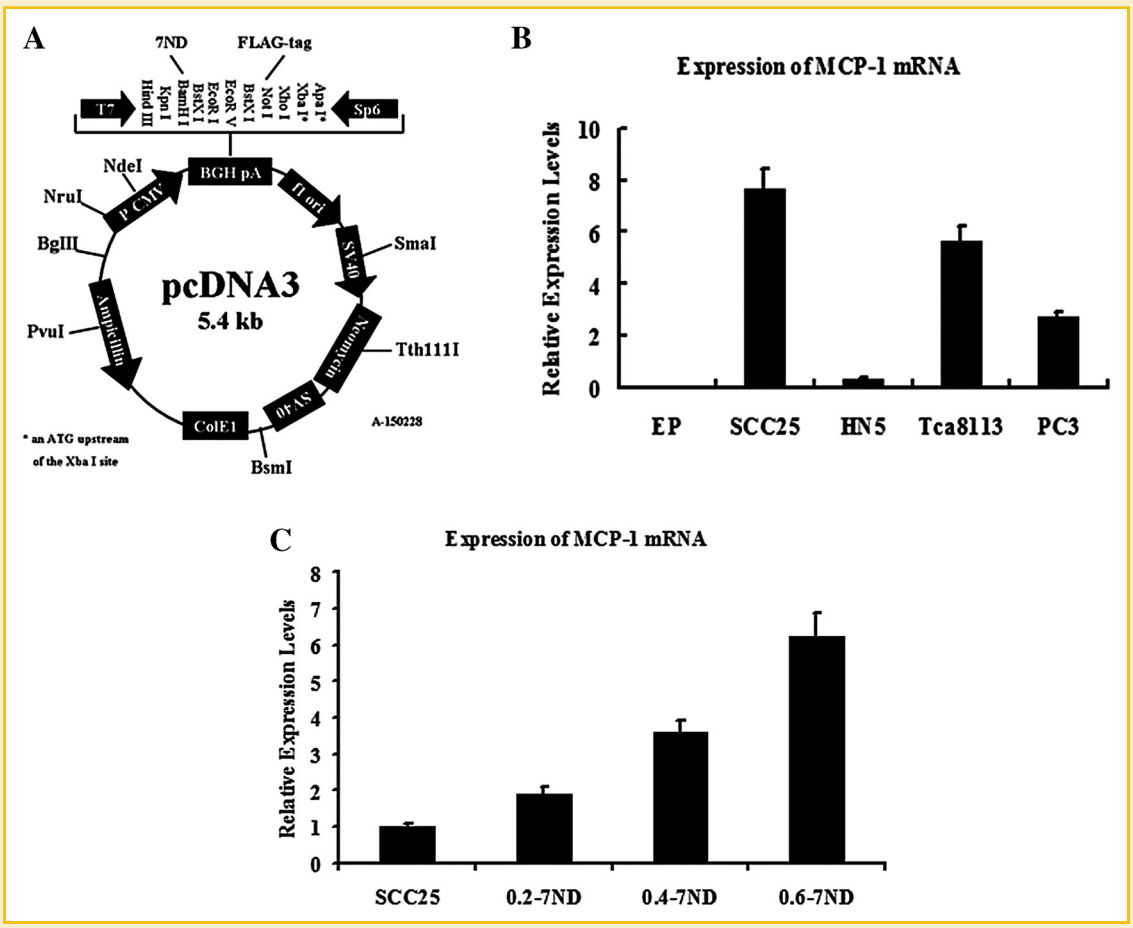

Fig. 2. The 7ND vector was transfected into SCC25 cells and a stabilized cell line was constructed. (A) The structure of the 7ND vector. (B) Expression of MCP-1 mRNA in cell lines of OSCC (SCC25, HN5, and Tca8113), the cell line SCC25 had the highest expression of MCP-1 mRNA. EP cells served as the negative control while PC3 cells were used as the positive control. (C) Real-time PCR was used to confirm the expression of MCP-1 mRNA in stabilized cells: SCC25 cells with 0.6 μg of 7ND vector (SCC25-7ND) had the highest expression of MCP-1 mRNA. Data were shown as mean ± SD of three independent experiments.

as follows: Group 1. $CD14^+$ monocytes with CSF1 (25 ng/mL) and RANKL (40 ng/mL); Group 2. $CD14^+$ monocytes with CSF1 (25 ng/mL) and RANKL (40 ng/mL), plus 10% (v/v) CM of SCC25 cells; Group 3. $CD14^+$ monocytes with CSF1 (25 ng/mL) and RANKL (40 ng/mL), plus 10% (v/v) CM of SCC25-7ND cells; Group 4. $CD14^+$ monocytes with CSF1 (25 ng/mL) and RANKL (40 ng/mL), plus the neutralization anti-MCP-1 antibody. CM was collected as follows: cells were washed with PBS and then the medium was changed into α-MEM without FBS. After 48 h culture, the entire medium was collected and centrifuged at 1,500 g, for 20 min at 4 °C to remove any cell debris. After these monocytes had been cultured under the same condition for seven days, osteoclasts were formed: these were subsequently fixed in 10% formaldehyde solution and stained for TRAP. TRAP positive cells that had three or more nuclei were considered to be multinucleated osteoclasts. Hoechst staining (Cellomics, Pittsburgh, PA) was used to visualize nuclei. Rhodamine-conjugated phalloidin (Life Technologies) was used to stain for F-actin. Four fields were randomly selected and counted for osteoclast and F-actin numbers by two independent assessors.

IN VIVO ANIMAL MODEL OF BONE INVASION BY OSCC

Balb-c nude mice were purchased from Animal Resources Centre (ARC, Australia). These mice were housed in the animal facility of Griffith University Gold Coast Campus, and cared by the animal

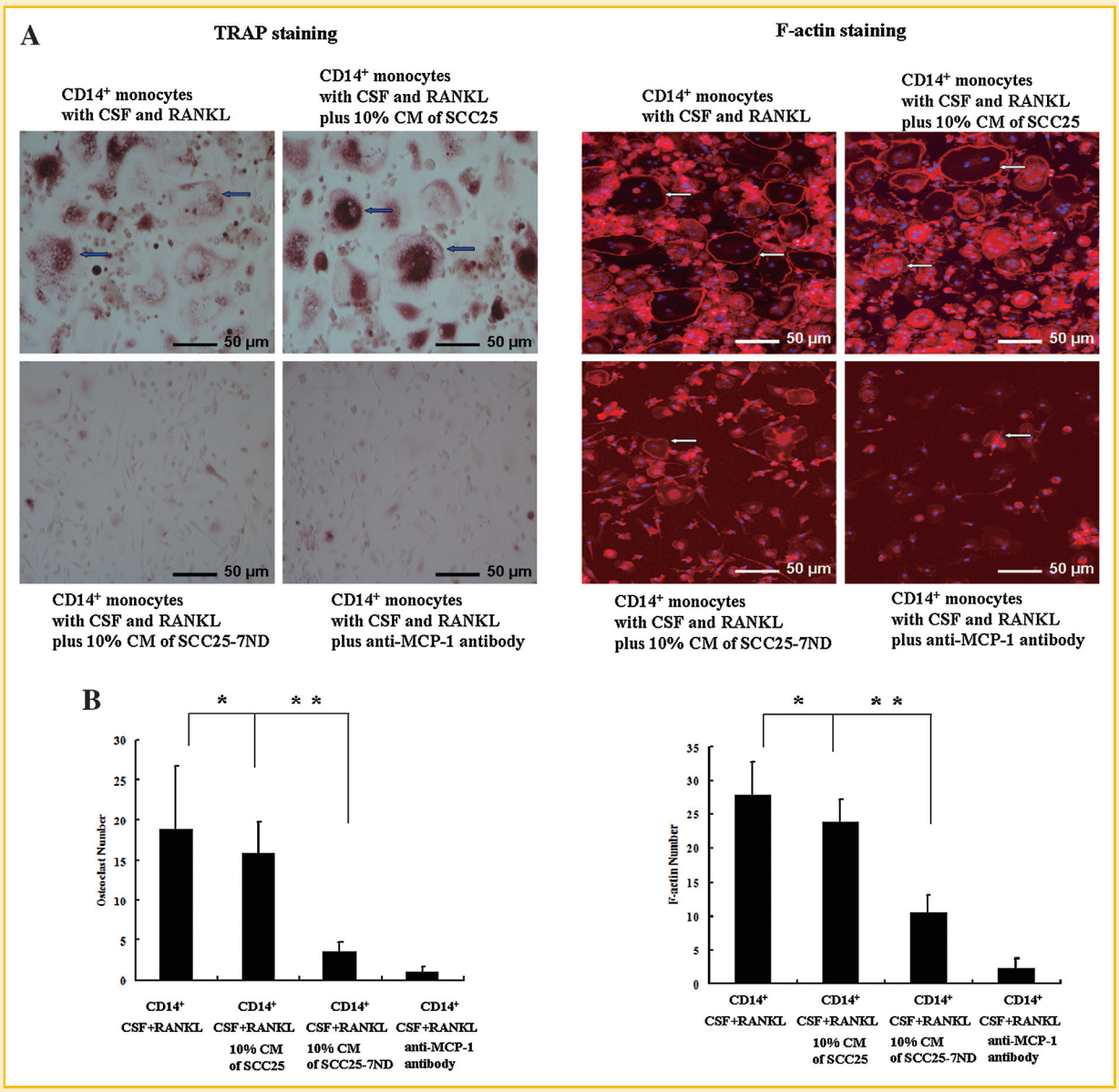

Fig. 3. 10% CM of SCC25-7ND cells efficiently inhibited the formation of human osteoclasts generated from $CD14^+$ monocyte subpopulation. (A) TRAP staining showed significantly fewer osteoclasts were found in the group treated with 10% CM (v/v) of SCC25-7ND cells (arrow, bar = 50 μm); Immunofluorescence suggested similar results, and significantly less F-actin staining was observed in the group treated with 10% CM (v/v) of SCC25-7ND cells (arrow, bar = 50 μm). (B) Quantification of osteoclast or F-actin numbers was performed with 4 fields randomly selected. Data were shown as mean ± SD of three independent experiments (*, $P > 0.05$; **, $P < 0.05$).

house staff. All protocols were reviewed and approved by Griffith University Ethics Committee (MSC/06/11/AEC). At 6–7 weeks of age, these mice were used to develop a model of bone invasion by OSCC in vivo. Under sterile conditions, OSCC cells (6×10^6/100 μL) were injected subcutaneously overlaying the calvariae. Mice were randomly divided into three groups (n = 6/group): the negative control group received PBS (Group 1); the positive control group received cells of SCC25 (Group 2); the experimental group received cells of SCC25-7ND (Group 3). All animals were sacrificed after six weeks. Tumors and calvariae were surgically removed and fixed in 4% paraformaldehyde (PFA, Sigma) for histological and immunohistochemical analysis.

MICRO-COMPUTED TOMOGRAPHY (μCT) IMAGING

Calvariae were surgically removed from PBS treated control, SCC25, SCC25-7ND tumors-bearing nude mice, fixed in 70% ethanol and scanned using a μCT instrument (SCANCO Medical AG, Brüttisellen, Switzerland). μCT-Analyser software (from μCT) was used to analyse the structure of the samples using the global segmentation method. Two-dimensional images were used to generate three-dimensional reconstructions with the software supplied with the instrument. The area of each calvaria was outlined for analysis and quantification, the amount of bone resorbed was determined as the percentage of resorption bone volume occupied by total bone volume.

FLOW CYTOMETRY ANALYSIS

Bone marrow cells (BMCs) from mice in each group were taken out from tibia on Week 6. The CD14 subpopulation of BMCs were evaluated by incubating 1×10^6 cells with the anti-CD14 antibody in PBS at 4 °C for 30 min. Thereafter, cells were stained with PE-conjugated rat anti-mouse secondary antibody. Flow cytomery analysis (FACS) was carried out on a FACScan flow cytometer (BD). The unstained cells were gated out and data acquisition with analysis was performed using CellQuest software (BD).

HISTOLOGIC AND IMMUNOHISTOCHEMICAL ANALYSIS

PFA-fixed tumor samples collected from these nude mice in different groups were processed for paraffin sectioning. Serial 5 μm sections was cut on Leica RM 2235 rotary microtome (Leica Microsystems, Canada) and stained with haematoxylin and eosin (H&E). Immunohistochemical staining of the sections was performed by incubation of serial sections with the primary antibody of MCP-1 (1:80) overnight followed by HRP labelled secondary antibody and DAB staining. Specimens treated with non-immune serum served as

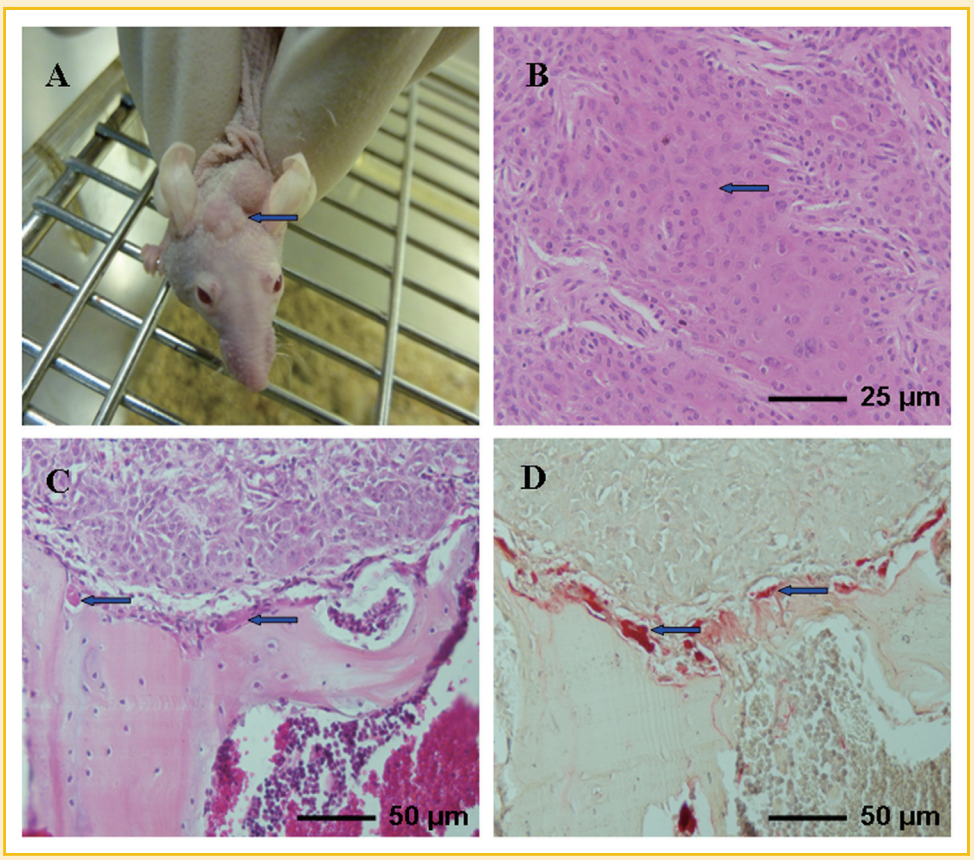

Fig. 4. Establishment of the animal model (3 nude mice) of bone invasion by OSCC cells. (A) Tumour formed in one week, localized in the area of calvaria (arrow, photos taken on Week 2 of tumour development). (B–C) H&E staining showed well-differentiated SCC was grown and invaded the adjacent bone tissue (arrow, bar = 25/50 μm). (D) Numerous osteoclasts were stained by TRAP (red) and found in the tumour–bone interface (arrow, bar = 50 μm).

control. To perform histochemical staining for these tumor-bearing calvariae, all calvariae were decalcified in 10% EDTA (pH = 7.4) for two weeks and processed for paraffin embedding. Serial 5 μm sections of paraffin embedded calvariae were stained by both H&E and TRAP. Histomorphometric analysis of TRAP-positive osteoclast numbers at the tumor-bone interface was performed. For each section, an area of 2 mm^2 with the tumor-bone interface was defined for counting osteoclast numbers. Four fields of this area were randomly selected and counted to determine the numbers of TRAP-postitive osteoclasts.

STATISTIC ANALYSIS

Data analysis was performed using the SPSS software (SPSS 20.0, IBM). Student *t*-test was used to compare two means. One way analysis of variance (ANOVA) is applied to compare two or more means, followed by Student–Newan–Keuls (S–N–K) test. A *P* value of less than 0.05 was regarded as significant.

RESULTS

STRONG STAINING OF MCP-1 PROTEIN WAS FOUND IN TISSUE SAMPLES FROM OSCC PATIENTS WITH BONE INVASION

Sections of OSCC samples from 10 patients with bone invasion were investigated for the expression of MCP-1. Immunohistochemistry (IHC) showed that MCP-1 protein was strongly stained in cytoplasm of osteoclasts and tumor cells (Fig. 1A). Control sections were negative. A summary of the staining results was shown in Figure 1B.

STABILIZED SCC25 CELLS WITH 7ND VECTOR WERE GENERATED AFTER ANTIBIOTIC SELECTION

The 7ND vector was engineered by inserting 7ND sequence into the pcDNA3 vector (Invitrogen), where it was ligated into the BamHI and NotI restriction sites within the polylinker region (Fig. 2A). It also contains a G418/neomycin resistance cassette for antibiotic

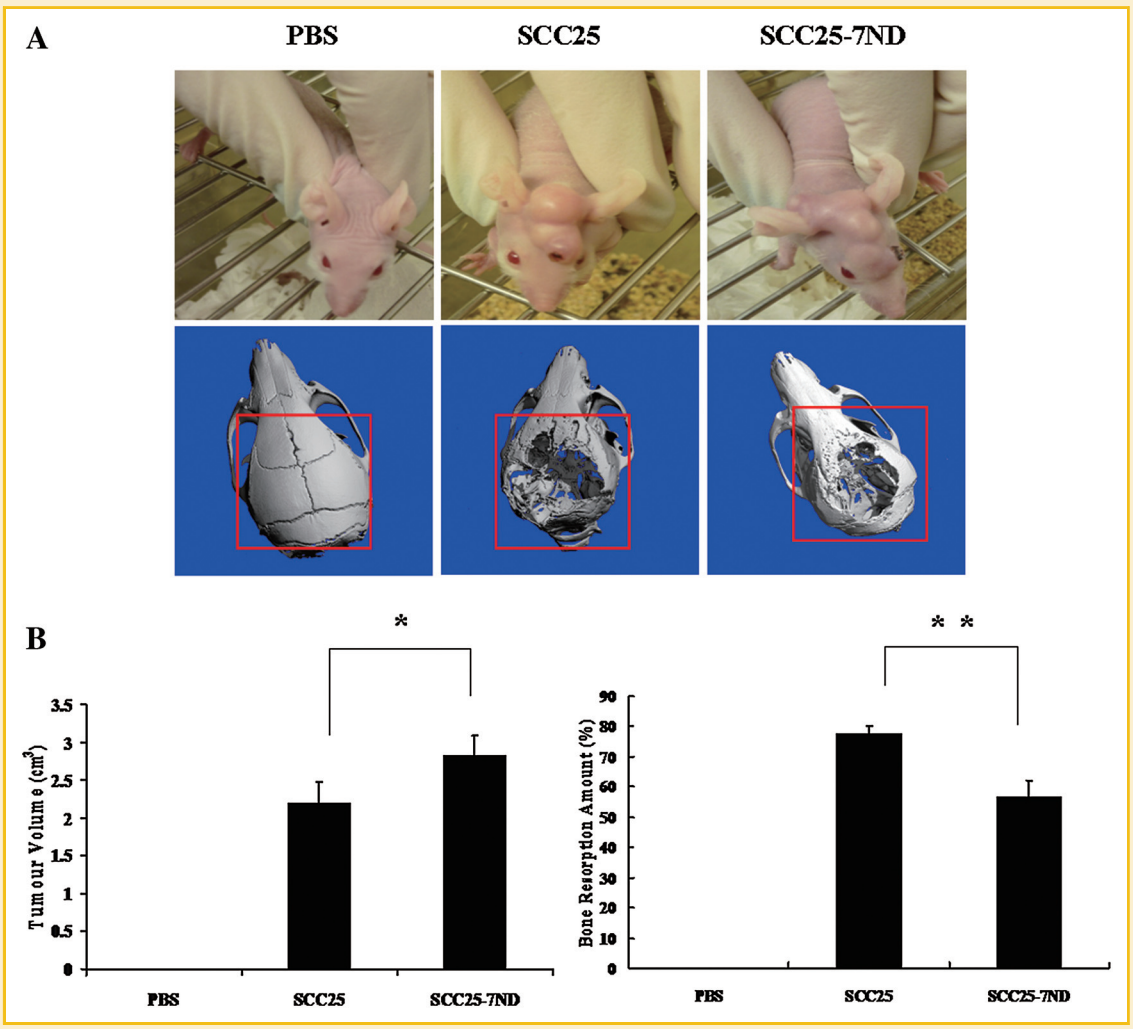

Fig. 5. μCT analysis of the bone resprotion area of calvariae with cells of SCC25 or SCC25–7ND. (A) Representative photos of tumour formation were taken on Week 6, and the same area of calvariae was outlined for analysis. (B) Quantification of the tumour volume (width × length × depth) and bone resorption amount. The average tumour volume of SCC25–7ND group was slightly bigger than SCC25 group (*, $P > 0.05$), while significantly smaller amount of resorbed bone was found in calvariae with OSCC cells of SCC25–7ND (**, $P < 0.05$). PBS injection served as negative control with an intact area of calvariae. Data were shown as mean ± SD of six mice for each group.

selection. Real-time PCR showed that MCP-1 mRNA was highly expressed by 3 different cell lines of OSCC (SCC25, HN5, Tca8113), and the cell line of SCC25 had the highest expression (Fig. 2B). Three concentrations of 7ND vector (0.2 μg, 0.4 μg, 0.6 μg) were used to transfect SCC25 cells, and stabilized cells with 7ND vector were selected by 0.3 mg/mL of G418. Since primers of MCP-1 can amplify mRNA of 7ND, Real-time PCR was used to detect the relative gene expression of MCP-1 in all transfected cells. Results showed that SCC25 cells with 0.6 μg of 7ND vector (SCC25-7ND) had the highest expression of MCP-1 (Fig. 2C).

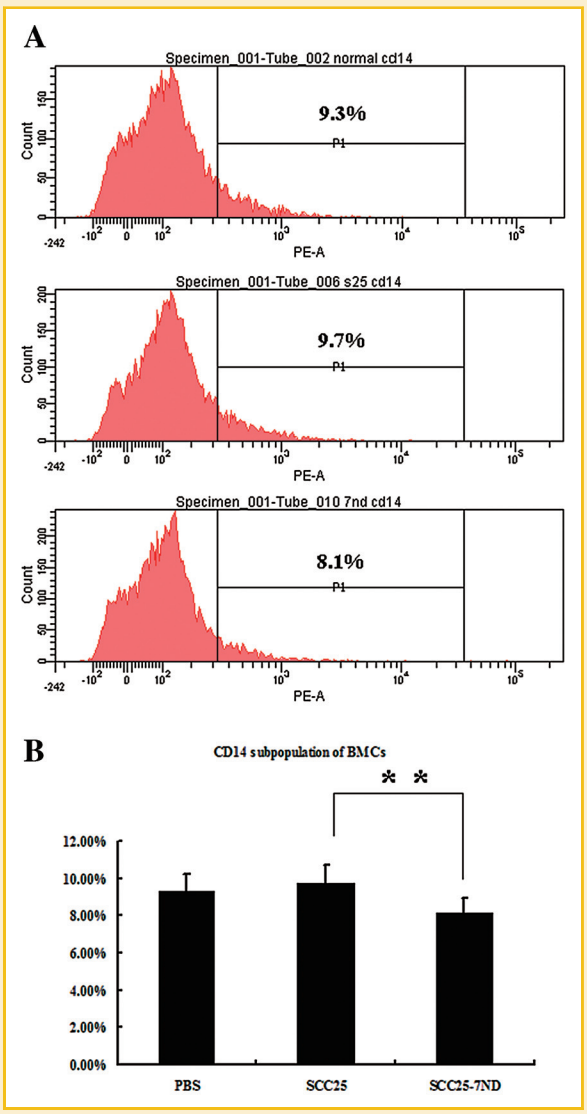

Fig. 6. FACS analysis of the $CD14^+$ subpopulation of BMCs in nude mice. Results showed that $CD14^+$ subpopulation of BMCs was slightly reduced in mice injected with SCC25-7ND cells (8.1%), comparing with mice received injection with SCC25 cells (9.7%) (**, $P < 0.05$). $CD14^+$ subpopulation of BMCs from normal mice with PBS injection served as the negative control (9.3%). These results represented three independent experiments of six mice for each group.

10% CM OF SCC25-7ND CELLS EFFICIENTLY INHIBITED THE FORMATION OF HUMAN OSTEOCLASTS OBTAINED FROM $CD14^+$ MONOCYTE SUBPOPULATION

The $CD14^+$ monocyte subpopulation was extracted from PBMCs using CD14 microbeads, and osteoclasts were grown from these monocytes with cytokines of CSF1 and RANKL. TRAP staining showed significantly fewer osteoclasts were found when treated with 10% CM of SCC25-7ND cells, comparing with 10% CM of SCC25 cells (Fig. 3A–B, $P < 0.05$). Immunofluorescence suggested similar results, and significantly less staining of F-actin was observed in those osteoclasts treated with 10% CM of SCC25-7ND cells (Fig. 3A–B, $P < 0.05$). The neutralization antibody against MCP-1 was also used for osteoclast generation, and nearly no osteoclasts were found in this positive control group.

THE ANIMAL MODEL OF BONE INVASION BY OSCC WAS ESTABLISHED BY INJECTING TUMOUR CELLS ONTO THE SURFACE OF CALVARIAE OF NUDE MICE

A trial with three nude mice was carried out to confirm the injection sites. Cells of SCC25 were injected onto the surface of calvariae where macroscopic tumours formed in one week (Fig. 4A, photos taken on Week 2). H&E staining of paraffin sections of these tumours showed well-differentiated SCCs (Fig. 4B), invading the adjacent bone tissue (Fig. 4C). Numerous osteoclasts were stained by TRAP and found at the tumour-bone interface (Fig. 4D).

μCT ANALYSIS OF RESORPTION AREA OF CALVARIAE WITH OSCC CELLS OF SCC25 OR SCC25-7ND

Tumor volume (width × length × depth) was recorded on Week 6, and data showed the average tumour volume of SCC25-7ND group was slightly bigger than SCC25 group (Fig. 5A–B, $P > 0.05$). μCT analysis suggested that significantly smaller amount of bone resorbed was found in calvariae with OSCC cells of SCC25-7ND, comparing with cells of SCC25 (Fig. 5A–B, $P < 0.05$). PBS injection served as the negative control, where all calvariae showed intact area.

THE $CD14^+$ SUBPOPULATION OF BMCs WAS REDUCED IN MICE INJECTED WITH CELLS OF SCC25-7ND

FACS analysis showed the $CD14^+$ subpopulation of BMCs was slightly reduced in mice injected with SCC25-7ND cells (8.1%, Fig. 6), in comparison to those mice who received injection with SCC25 cells (9.7%, Fig. 6). This difference is statistically significant ($P < 0.05$).

MCP-1 PROTEIN WAS MAINLY LOCATED IN THE CYTOPLASM OF TUMOUR CELLS FOR BOTH GROUPS

H&E staining showed that well-differentiated SCC formed in both groups, after injection with cells of SCC25 or SCC25-7ND (Fig. 7). IHC was performed to locate the MCP-1 protein. This was mostly found in the neoplastic cells, mainly located in the cytoplasm and cell membrane, while less staining was found in nuclei (Fig. 7).

SIGNIFICANTLY FEWER OSTEOCLASTS WERE FOUND IN THE BONE RESORPTION LACUNAE WITH CELLS OF SCC25-7ND IN COMPARISON TO CELLS OF SCC25

H&E staining of both groups showed squamous epithelial OSCC cells invading bone, with many osteoclasts accumulating in typical

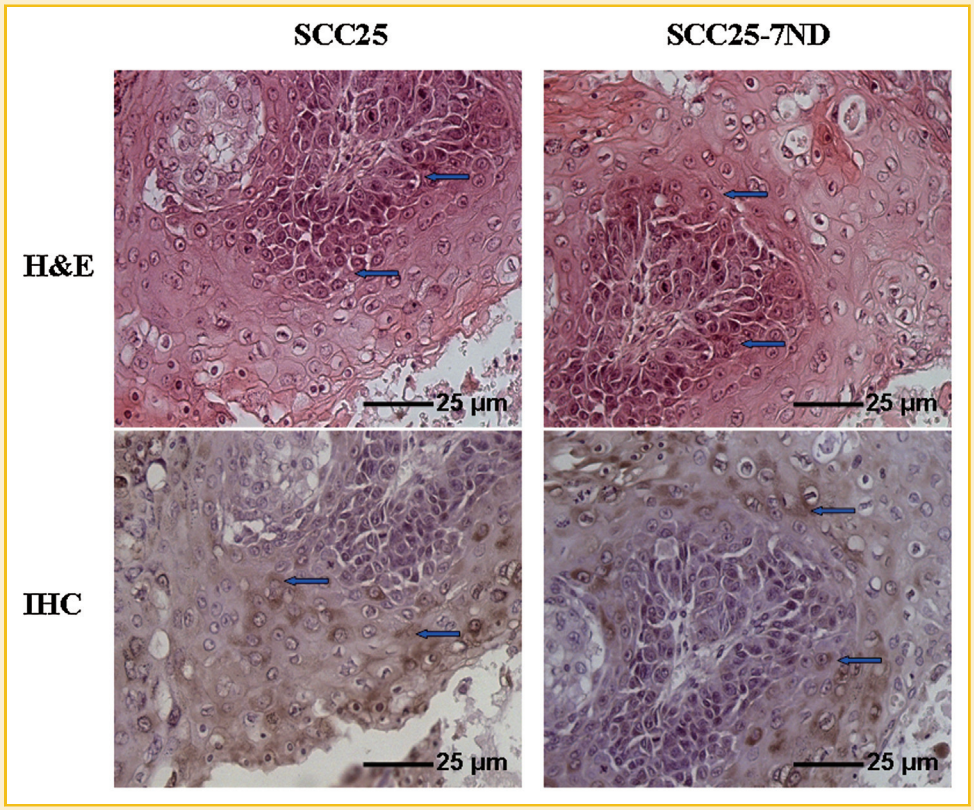

Fig. 7. Staining of MCP-1 protein in tumour cells of both groups. H&E staining showed well-differentiated squamous cell carcinoma (SCC) was formed in mice of both groups, after injection of both SCC25 or SCC25-7ND cells (arrow, H&E, bar = 25 μm). IHC further confirmed that MCP-1 protein was mainly located in cytoplasm and membrane of OSCC cells (arrow, DAB, bar = 25 μm).

resorption lacunae (Fig. 8A). TRAP staining was used to locate and count osteoclasts. Fewer osteoclasts were found in resorption lacunae with cells of SCC25-7ND, comparing with cells of SCC25. There were significant differences between these two groups for osteoclast numbers (Fig. 8B, $P < 0.05$).

DISCUSSION

To the best of our knowledge, this is the first report providing information concerning the relationship between MCP-1 and bone invasion by OSCC. The progression of OSCC is related to the expression of chemokines, the concentration of CXCL8, CXCL10, and CCL14 were found to be significantly elevated in oral fluids of patients with OSCC, comparing with patients of periodontitis, suggesting the chemokine profile of OSCC patients might be a useful parameter in clinical practice [Michiels et al., 2009]. MCP-1, a major attractant of leukocytes, was produced by various cell lines of OSCC in vitro, and increased in oral fluids and tissues from patients with OSCC in vivo [Chen et al., 2011]. However, little is known as to whether or not MCP-1 plays a critical role in the progression of bone invasion by OSCC. A recent study reported patients of nasopharyngeal carcinoma with extensive invasion of the skull base had higher concentrations of CCL2 and TNF-α in serum than those without, or with only small invasion, indicating the potential value of MCP-1 as a target for inhibition [Lu et al., 2011]. In the present study, MCP-1 protein was examined in human tissue samples using IHC, which showed MCP-1 was strongly stained by both osteoclasts and tumour cells. The expression of MCP-1 mRNA was also detected in three different cell lines of OSCC, all of which expressed MCP-1, especially the cell line SCC25. It was reported 0.23% of side population (SP) cells could be isolated form SCC25 cultures: these possess the characteristics of cancer stem cells, such as higher proliferation rates and colony formation ability, indicating their invasive potential [Yanamoto et al., 2011]. The reasons why HN5 has relatively low expression of MCP-1 mRNA are currently unknown. Actually, cells of SCC25, HN5 and Tca8113 are OSCC cell lines with distinct properties, which generated from different primary sites of OSCC patients [Kalinowski et al., 2012]. In our previous study [Quan et al., 2013], these cells were found to have various abilities of invasion related with bone invasion of OSCC. Taking these observations into consideration, and given the high expression of MCP-1 in SCC25 cells, we selected these for the subsequent inhibitory studies.

7ND is an N-terminal deletion mutant of MCP-1, which lacks amino acids 2–8 and acts as a dominant-negative inhibitor of MCP-1 [Zhang et al., 1994]. Specifically, 7ND and wild-type MCP-1 form a heterodimer, which binds to the MCP-1 receptor (CCR2) and completely inhibits the monocyte chemotaxis mediated by MCP-1

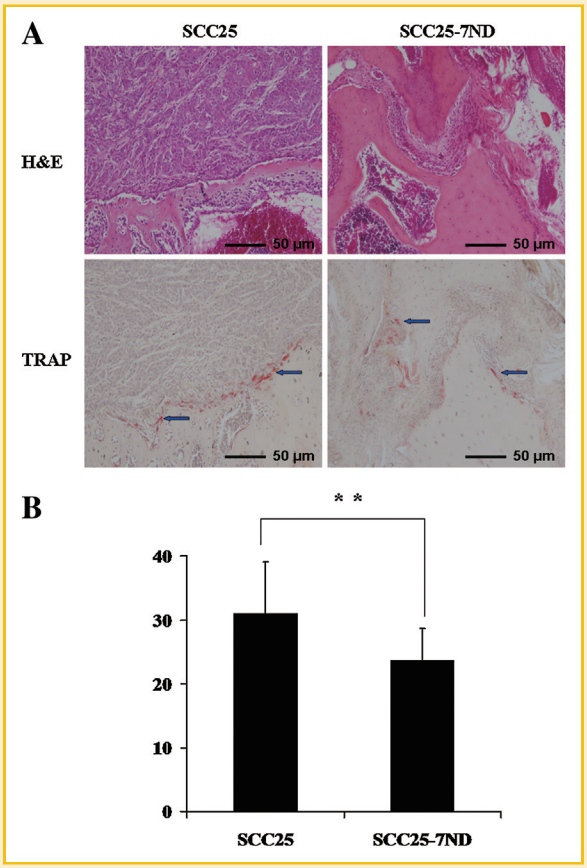

Fig. 8. The number of osteoclasts in tumour–bone interface. (A) H&E staining of both groups showed OSCC cells invaded the bone tissue, with many osteoclasts accumulating in typical resorption lacunae (bar = 50μm). TRAP staining was used to locate and count the osteoclasts of all samples (arrow, bar = 50 μm). (B) Results of quantification suggested significantly fewer osteoclasts were found in resorption lacunae with cells of SCC25–7ND, comparing with cells of SCC25 (**, $P < 0.05$). Data were shown as mean ± SD of 5 sections for one mice of each group.

in vitro [Zhang and Rollins, 1995]. Thus, it is possible to use 7ND like an antibody to block the expression of MCP-1 within gene therapy. For example, transfection of 7ND into skeletal muscle is an established strategy for gene therapy of anti-MCP-1 [Aoki et al., 2009]. Based on these reports, stabilized SCC25 cells with the 7ND vector were generated by antibiotic selection with G418, and CM of both SCC25 and SCC25-7ND cells was collected to observe whether these CM could work differently on human osteoclasts. After six days of culture, TRAP staining showed many osteoclasts formed in the group with 10% CM of SCC25 cells, which is consistent with a recent study that, CM of SCC25 could induce the formation of osteoclasts cultured from murine bone marrow cells in vitro [Martin et al., 2012]. Conversely, in the group with 10% CM of SCC25–7ND cells, it was observed that fewer osteoclasts formed. Therefore, these results suggest 7ND protein has been released into the CM and inhibited the formation of human osteoclasts in vitro. Similarly, a recent report of our group showed 10% CM from HEK293T cells transfected with 7ND expression construct strongly inhibited human osteoclast formation from PBMCs [Morrison et al., 2014]. Moreover, 100 ng/mL of 7ND peptide, purified from large amounts of transfected cell culture medium by FLAG affinity chromatography, was demonstrated to prevent RANKL mediated induction of NFATc2, CALM1 and transfection factor JUN.

To further prove the hypothesis, an animal model of bone invasion by OSCC was established to check whether 7ND would succeed in vivo. This "calvaria-injection" model is attractive for it is easy to inject OSCC cells onto the surface of calvaria of nude mice [Pandruvada et al., 2010]. Comparing with other animal models reported [Henson et al., 2007; Nomura et al., 2007], this model has the distinct advantage of causing animal limited stress, as there is no interference with mastication. Through histological studies, it was found that the tumours formed were moderately differentiated SCCs, which invading the bone, with plenty of osteoclasts lining on the edge of resorbed bone. The formal experiments were performed utilizing this model, with three groups of six mice in each group. μCT analysis found the bone resorption amount of the SCC25-7ND group was smaller than the SCC25 group. FACS was used to compare the CD14 subpopulation of BMCs between these two groups, and showed this population was reduced in mice with cells of SCC25-7ND. The differences between these two groups are small (8.1% vs 9.7%). This may be caused by the small number of animals (n = 6) for each group, or because the transfection system leads to limited amounts of 7ND protein circulating into the bloodstream. However, consistent with previous report of 7ND in vivo [Koga et al., 2008; Aoki et al., 2009], these results indicate that 7ND protein has circulated in the blood and competed with MCP-1, and this does inhibit monocytes being recruited into the bone marrow. Moreover, the histological and immonohistological analysis demonstrated that significantly fewer osteoclasts were found in the bone resorption lacunae of the SCC25-7ND group, comparing with the SCC25 group. All these results suggest 7ND protein has worked in vivo as studies in vitro. Other possible mechanism of 7ND inhibiting osteoclastogenesis such as 7ND has apoptotic effects on osteoclasts, is currently unclear and still under investigation. Sul et al described aberrant actin rings in osteoclasts from bone marrow-derived macrophages of MCP-1 knock out mice, which might be related to reduced levels of ERK, Akt, Rac1, and Rho [Sul et al., 2012]. Whether 7ND inhibits osteoclast generation via targeting on these factors needs to be further explored.

For a long time observation with the chemokine MCP-1, our group precisely demonstrated MCP-1 is induced by RANKL and promotes osteoclast fusion, defining a cell fate switch for osteoclast differentiation, suggest a role for chemokine signalling within osteoclast physiology [Kim et al., 2005; Kim et al., 2006]. Using an ulnar stress facture (SFx) model, which allows investigation of focal remodelling with a known time course and anatomical location, MCP-1 was specifically regulated during the early phase of remodelling after SFx initiation [Wu et al., 2013]. In addition, following daily injection of parathyroid hormone (PTH), MCP-1 knockout mice showed less trabecular bone mineral density and bone volume compared with wild-type mice, proving that MCP-1 is a key molecular mediator for the anabolic effects of PTH on bone [Tamasi et al., 2013]. Moreover, the present study has explored roles of MCP-1 in the progression of bone invasion by OSCC, showed the

relevance of MCP-1 to research on bone invasion by OSCC. Collectively, all these researches indicate that MCP-1 is a reasonable clinical target for blocking osteoclast differentiation, and support MCP-1 as a potential target for future gene therapy, as well as therapies of cancer, neuroinflammation and cardiovascular diseases [Chan et al., 2012; Rutar et al., 2012]. Future work will focus on how MCP-1 regulates early differentiation of osteoclasts and the signalling pathways involved, which may help to better understand the progression of this common complication of oral cancer in patients so afflicted.

ACKNOWLEDGMENT

We would like to thank Mr. Usman Khan, Mrs. Nikki Forzard and Dr. Koichi Ito for their technical assistance during the experiments.

REFERENCES

Aoki T, Kataoka H, Ishibashi R, Nozaki K, Egashira K, Hashimoto N. 2009. Impact of monocyte chemoattractant protein-1 deficiency on cerebral aneurysm formation. Stroke 40:942–951.

Balkwill FR. 2012. The chemokine system and cancer. J Pathol 226:148–157.

Baron R, Ferrari S, Russell RG. 2011. Denosumab and bisphosphonates: Different mechanisms of action and effects. Bone 48:677–692.

Bektas-Kayhan K, Unur M, Boy-Metin Z, Cakmakoglu B. 2012. MCP-1 and CCR2 gene variants in oral squamous cell carcinoma. Oral Dis 18:55–59.

Chan CT, Moore JP, Budzyn K, Guida E, Diep H, Vinh A, Jones ES, Widdop RE, Armitage JA, Sakkal S, Ricardo SD, Sobey CG, Drummond GR. 2012. Reversal of vascular macrophage accumulation and hypertension by a CCR2 antagonist in deoxycorticosterone/salt-treated Mice. Hypertension 60:1207–1212.

Charo IF, Ransohoff RM. 2006. The many roles of chemokines and chemokine receptors in inflammation. N Engl J Med 354:610–621.

Chen MK, Yeh KT, Chiou HL, Lin CW, Chung TT, Yang SF. 2011. CCR2-64I gene polymorphism increase susceptibility to oral cancer. Oral Oncol 47:577–582.

Costa-Rodrigues J, Fernandes A, Fernandes MH. 2011. Spontaneous and induced osteoclastogenic behaviour of human peripheral blood mononuclear cells and their CD14(+) and CD14(−) cell fractions. Cell Prolif 44:410–419.

Deshmane SL, Kremlev S, Amini S, Sawaya BE. 2009. Monocyte chemoattractant protein-1 (MCP-1): An overview. J Interferon Cytokine Res 29:313–326.

Faccio R. 2011. Immune regulation of the tumor/bone vicious cycle. Ann N Y Acad Sci 1237:71–78.

Hemingway F, Cheng X, Knowles HJ, Estrada FM, Gordon S, Athanasou NA. 2011. In vitro generation of mature human osteoclasts. Calcif Tissue Int 89:389–395.

Henson B, Li F, Coatney DD, Carey TE, Mitra RS, Kirkwood KL, D'Silva NJ. 2007. An orthotopic floor-of-mouth model for locoregional growth and spread of human squamous cell carcinoma. J Oral Pathol Med 36:363–370.

Kalinowski FC, Giles KM, Candy PA, Ali A, Ganda C, Epis MR, Webster RJ, Leedman PJ. 2012. Regulation of epidermal growth factor receptor signaling and erlotinib sensitivity in head and neck cancer cells by miR-7. PLoS One 7: e47067.

Kim MS, Day CJ, Morrison NA. 2005. MCP-1 is induced by receptor activator of nuclear factor-{kappa}B ligand, promotes human osteoclast fusion, and rescues granulocyte macrophage colony-stimulating factor suppression of osteoclast formation. J Biol Chem 280:16163–16169.

Kim MS, Day CJ, Selinger CI, Magno CL, Stephens SR, Morrison NA. 2006. MCP-1-induced human osteoclast-like cells are tartrate-resistant acid phosphatase, NFATc1, and calcitonin receptor-positive but require receptor activator of NFkappaB ligand for bone resorption. J Biol Chem 281:1274–1285.

Koga M, Kai H, Egami K, Murohara T, Ikeda A, Yasuoka S, Egashira K, Matsuishi T, Kai M, Kataoka Y, Kuwano M, Imaizumi T. 2008. Mutant MCP-1 therapy inhibits tumor angiogenesis and growth of malignant melanoma in mice. Biochem Biophys Res Commun 365:279–284.

Lu X, Kang Y. 2009. Chemokine (C-C motif) ligand 2 engages CCR2+ stromal cells of monocytic origin to promote breast cancer metastasis to lung and bone. J Biol Chem 284:29087–29096.

Lu X, Qian CN, Mu YG, Li NW, Li S, Zhang HB, Li SW, Wang FL, Guo X, Xiang YQ. 2011. Serum CCL2 and serum TNF-α–two new biomarkers predict bone invasion, post-treatment distant metastasis and poor overall survival in nasopharyngeal carcinoma. Eur J Cancer 47:339–346.

Martin CK, Dirksen WP, Shu ST, Werbeck JL, Thudi NK, Yamaguchi M, Wolfe TD, Heller KN, Rosol TJ. 2012. Characterization of bone resorption in novel in vitro and in vivo models of oral squamous cell carcinoma. Oral Oncol 48:491–499.

Michiels K, Schutyser E, Conings R, Lenaerts JP, Put W, Nuyts S, Delaere P, Jacobs R, Struyf S, Proost P, Van Damme J. 2009. Carcinoma cell-derived chemokines and their presence in oral fluid. Eur J Oral Sci 117:362–368.

Mizutani K, Sud S, McGregor NA, Martinovski G, Rice BT, Craig MJ, Varsos ZS, Roca H, Pienta KJ. 2009. The chemokine CCL2 increases prostate tumor growth and bone metastasis through macrophage and osteoclast recruitment. Neoplasia 11:1235–1242.

Moreaux J, Hose D, Kassambara A, Reme T, Moine P, Requirand G, Goldschmidt H, Klein B. 2011. Osteoclast-gene expression profiling reveals osteoclast-derived CCR2 chemokines promoting myeloma cell migration. Blood 117:1280–1290.

Morrison NA, Day CJ, Nicholson GC. 2014. Dominant negative MCP-1 blocks human osteoclast differentiation. J Cell Biochem 115:303–312.

Ni W, Egashira K, Kitamoto S, Kataoka C, Koyanagi M, Inoue S, Imaizumi K, Akiyama C, Nishida KI, Takeshita A. 2001. New anti-monocyte chemoattractant protein-1 gene therapy attenuates atherosclerosis in apolipoprotein E-knockout mice. Circulation 103:2096–2101.

Nomura T, Shibahara T, Katakura A, Matsubara S, Takano N. 2007. Establishment of a murine model of bone invasion by oral squamous cell carcinoma. Oral Oncol 43:257–262.

Pandruvada SN, Yuvaraj S, Liu X, Sundaram K, Shanmugarajan S, Ries WL, Norris JS, London SD, Reddy SV. 2010. Role of CXC chemokine ligand 13 in oral squamous cell carcinoma associated osteolysis in athymic mice. Int J Cancer 126:2319–2329.

Quan J, Elhousiny M, Johnson NW, Gao J. 2013. Transforming growth factor-β1 treatment of oral cancer induces epithelial-mesenchymal transition and promotes bone invasion via enhanced activity of osteoclasts. Clin Exp Metastasis 30:659–670.

Quan J, Johnson NW, Zhou G, Parsons PG, Boyle GM, Gao J. 2012. Potential molecular targets for inhibiting bone invasion by oral squamous cell carcinoma: a review of mechanisms. Cancer Metastasis Rev 31:209–219.

Quan J, Zhou C, Johnson NW, Francis G, Dahlstrom JE, Gao J. 2012. Molecular pathways involved in crosstalk between cancer cells, osteoblasts and osteoclasts in the invasion of bone by oral squamous cell carcinoma. Pathology 44:221–227.

Rutar MV, Natoli RC, Provis JM. 2012. Small interfering RNA-mediated suppression of Ccl2 in Muller cells attenuates microglial recruitment and photoreceptor death following retinal degeneration. J Neuroinflammation 9:221.

Severin IC, Souza AL, Davis JH, Musolino N, Mack M, Power CA, Proudfoot AE. 2012. Properties of 7ND-CCL2 are modulated upon fusion to Fc. Protein Eng Des Sel 25:213–222.

Sul OJ, Ke K, Kim WK, Kim SH, Lee SC, Kim HJ, Kim SY, Suh JH, Choi HS. 2012. Absence of MCP-1 leads to elevated bone mass via impaired actin ring formation. J Cell Physiol 227:1619–1627.

Taddei SR, Andrade I, Jr , Queiroz-Junior CM, Garlet TP, Garlet GP, Cunha Fde, Teixeira Q, da Silva MM. 2012. Role of CCR2 in orthodontic tooth movement. Am J Orthod Dentofacial Orthop 141:153–160.

Tamasi JA, Vasilov A, Shimizu E, Benton N, Johnson J, Bitel CL, Morrison N, Partridge NC. 2013. Monocyte chemoattractant protein-1 is a mediator of the anabolic action of parathyroid hormone on bone. J Bone Miner Res 28:1975–1986.

Wu AC, Morrison NA, Kelly WL, Forwood MR. 2013. MCP-1 expression is specifically regulated during activation of skeletal repair and remodeling. Calcif Tissue Int 92:566–575.

Zhang YJ, Rutledge BJ, Rollins BJ. 1994. Structure/activity analysis of human monocyte chemoattractant protein-1 (MCP-1) by mutagenesis. Identification of a mutated protein that inhibits MCP-1-mediated monocyte chemotaxis. J Biol Chem 269:15918–15924.

Zhang Y, Rollins BJ. 1995. A dominant negative inhibitor indicates that monocyte chemoattractant protein 1 functions as a dimer. Mol Cell Biol 15:4851–4855.

Yanamoto S, Kawasaki G, Yamada S, Yoshitomi I, Kawano T, Yonezawa H, Rokutanda S, Naruse T, Umeda M. 2011. Isolation and characterization of cancer stem-like side population cells in human oral cancer cells. Oral Oncol 47:855–860.